SGG☆SGS sc|nat

CrossMark

Investigating distant effects of the Moesian promontory: brittle tectonics along the western boundary of the Getic unit (East Serbia)

Ana Mladenović[1] (ID) · Milorad D. Antić[2] · Branislav Trivić[1] · Vladica Cvetković[1]

Abstract

In this study, we report evidence for brittle deformation in a part of the Carpatho–Balkan orogen, which is explained in terms of effects of the rigid Moesian promontory of the European plate on fault kinematics in East Serbia. We focus on the westernmost part of the Getic Unit of the East Serbian Carpatho–Balkanides, i.e. the Gornjak–Ravanica Unit, located between two main thrusts that were repeatedly activated from Early Cretaceous to recent times. We combine a new data set on fault kinematics and tectonic paleostress tensors, with literature data about neotectonic and recent fault activity, in order to reconstruct brittle tectonic events that were active in this area since Oligocene times. Two brittle tectonic phases were distinguished. The older phase was most probably active from the Oligocene to the end of the middle Miocene, and was characterized by the activation of faults that accommodated a complex sequence of clockwise rotations of the Dacia mega-unit around the rigid Moesian promontory. The younger deformational phase most likely started in the late Miocene and is probably still active in recent time. It is characterized by strike-slip tectonics, resulting from the far-field stress generated by the collision of the Adriatic microplate, the Moesian promontory and the tectonic units in between. This stress field is shown to be highly heterogeneous even in the relatively small research area; local areas of transtension and transpression have also been very important in controlling the fault kinematics in the western part of the Getic Unit.

Keywords Getic unit · Moesian promontory · Carpatho-Balkan orogen · Brittle tectonics · Gornjak-Ravanica unit

1 Introduction

The Carpatho—Balkanides, together with the Dinarides, are part of a complex double-vergent orogen system that geomorphologically dominates in the central axis of the Balkan Peninsula. The Carpatho—Balkan—Dinaric orogenic system itself is part of a much wider, Alpine–Himalayan collisional orogen. The Carpatho–Balkan–Dinaric

✉ Ana Mladenović
ana.mladenovic@rgf.bg.ac.rs

1 Faculty of Mining and Geology, University of Belgrade, Đušina 7, Belgrade, Serbia

2 South Danube Metals, Bulevar Kralja Aleksandra 24, Belgrade, Serbia

orogenic system in the Balkans is the result of Mesozoic closure of the Neotethyan Ocean that existed in-between the Gondwana (Africa) and Eurasian (Europe) continental plates, and subsequent Cretaceous–Neogene collisional and post-collisional phases (Schmid et al. 2008; Cvetković et al. 2016; and references therein).

The East Serbian Carpatho–Balkanides consist of an east-vergent nappe-stack system that formed during late Early Cretaceous thrusting in the Europe-derived Dacia mega-unit (Schmid et al. 2008; Fig. 1). From west to east, the Carpatho–Balkanides comprise the following tectonic units: the structurally highest Serbo-Macedonian Massif together with the East Vardar ophiolites obducted on it, the Getic Unit and the structurally lowest Danubian Unit (Schmid et al. 2008; Kräutner and Krstić 2003). The entire region underwent compression until the Late Cretaceous, and as a result of ongoing compression clockwise rotation of the Dacia mega-unit around the rigid Moesian promontory started at the end of the Cretaceous (Fügenschuh and Schmid 2005). This clockwise rotation and oroclinal bending of the Dacia mega-unit around the
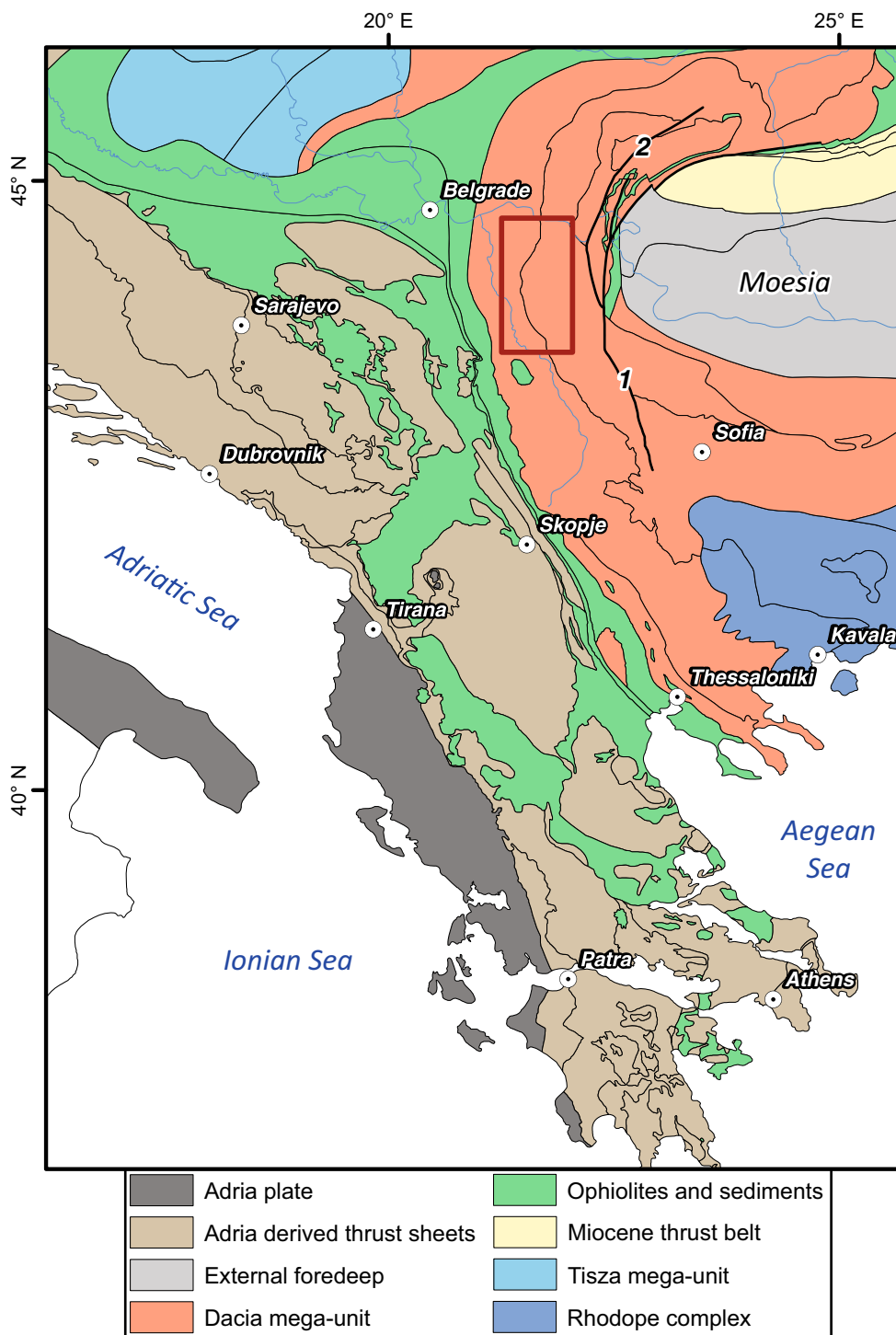
Ⓝ Birkhäuser

Fig. 1 Tectonic map of the Balkan peninsula (after Schmid et al. 2008). Main strike slip faults are marked with numbers: 1 Timok fault, 2 Cerna-Jiu fault. Red frame indicates the location of the working area

Moesian promontory was probably the main factor that controlled the tectonics in the East Serbian Carpatho–Balkanides in Cenozoic times. The rotation was accommodated by the formation of large strike-slip faults (Cerna-Jiu and Timok), which show a cumulative displacement of up to 100 km in the central (East Serbian) part of the orogen (Sikošek 1955; Schmid et al. 2008). During Miocene times the formation of small sedimentary basins started in this region. This was followed by renewed compression that reactivated older main thrusts/contacts of

the Cretaceous nappe stack of the Dacia mega-unit. Relative timing of Miocene extensional and younger, compressive tectonic phase, is evident by the fact that in some deep coal mines, located along the investigated area, there is evidence for thrusting of red Permian sandstones over lower Miocene lacustrine sediments (Maksimović 1956). However, the exact timing of these two tectonic phases and their relationship with the ongoing regional tectonics of the wider area are yet unclear or very poorly constrained. One of the main questions that raises about these tectonic phases is whether they were regionally important, or rather of local importance and due to the rotation of the Dacia mega-unit around Moesia.

The main aim of this work is to document brittle tectonic events in the western part of the Getic Unit, and to try to better understand the influence of the rigid Moesian promontory on fault kinematics in the area. We focus on the westernmost sub-unit of the Getic nappe system, the Gornjak–Ravanica Unit (Fig. 2) and present new data on fault kinematics, which allows for distinguishing at least two brittle deformation phases. Our results demonstrate that Oligocene to recent tectonics of this area was most probably controlled by the complex rotation of the Dacia mega-unit around rigid Moesia, which also caused local perturbations in the stress field.
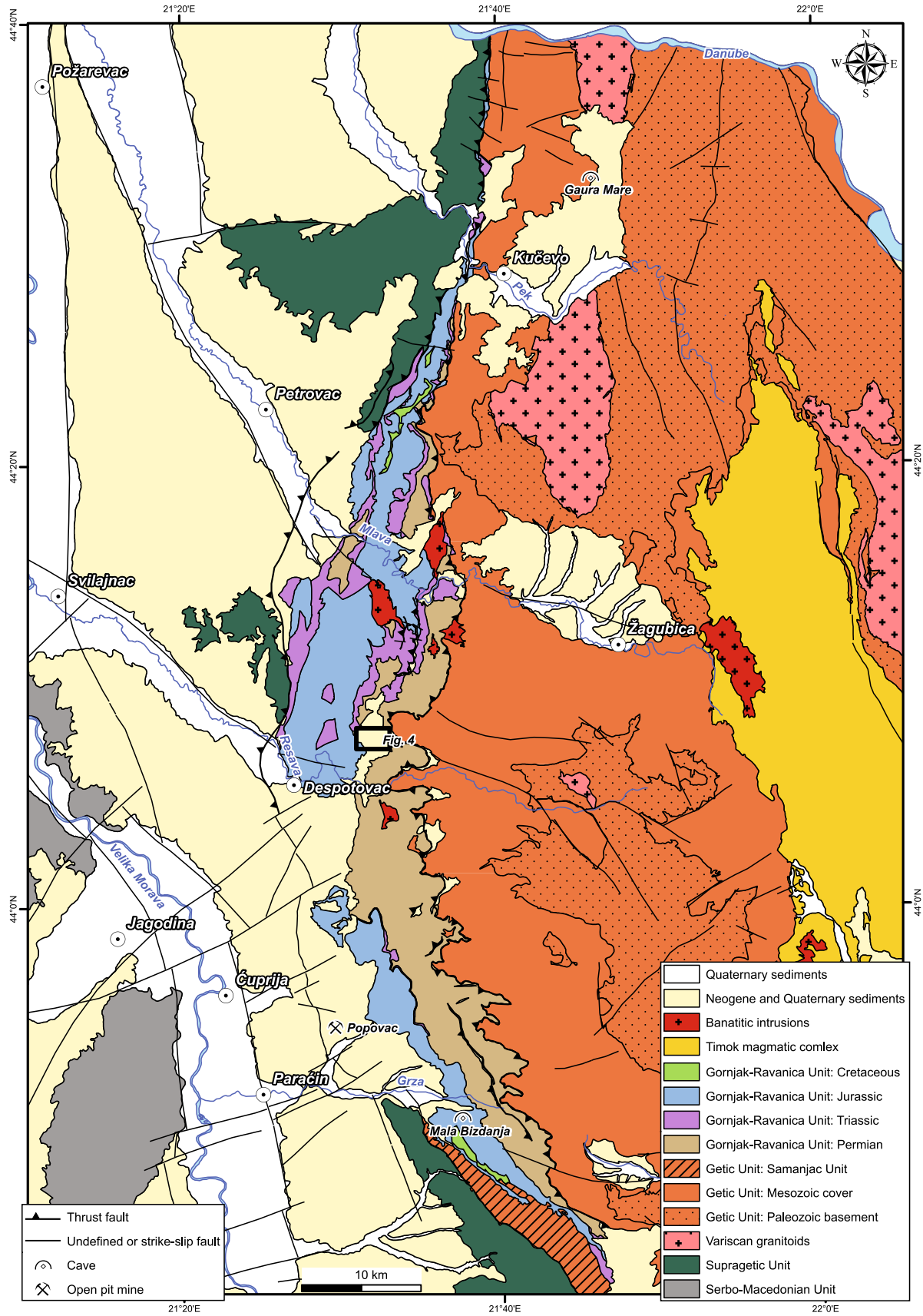
2 Geological setting

The Gornjak–Ravanica Unit (GRU; Dimitrijević 1997) is the westernmost thrust-sheet of the Getic nappe-stack within the Europe-derived Dacia mega-unit (Schmid et al. 2008; Figs. 1, 2). The GRU represents the Serbian part of the larger Saska-Gornjak and Resita units (Kräutner and Krstić 2003), that can be followed from Romania in the north, through Serbia, up to western Bulgaria in the southeast. The oldest rocks of the GRU are red Permian sandstones. In the central part, these Permian sandstones are covered by up to 100 m thick Lower Triassic "Scythian coloured sandstones". The so-called "Ravanica limestones" were deposited over the Lower Triassic in the central part of the research area (i.e. Dimitrijević 1997 and references therein). Middle Jurassic deposition started with conglomerates and quartz sandstones, that are covered by Bajocian sandy to clayey carbonates, oolitic limestones and shallow-neritic sandstones. These are followed by Callovian psammitic carbonates with abundant chert horizons indicating a slightly deeper marine environment (Banjac 2004 and references therein). Upper Jurassic sedimentation began with Kimmeridgian and Oxfordian facies of "limestones with chert", which are locally covered by reef limestones (Anđelković 1978). Deposition of carbonates continued with thick Tithonian reef and sub-reef limestones that are the most prominent rock type in the study area (Banjac 2004 and references therein). Mesozoic sedimentation ended with ca. 100 m thick Valanginian limestones, marls and shales, cropping out exclusively in the north of the research area (Dimitrijević 1997). Neogene sediments unconformably cover older rocks and are widespread in the Velika Morava basin situated west of the GRU (Fig. 2). These clastic sedimentary rocks were deposited in limnic, or fluvio-limnic environments from middle to upper Miocene times (Veselinović et al. 1970).

The GRU is in the footwall of the Serbo-Macedonian massif as evidenced by a thrust known as the "Morava dislocation" (Fig. 2). Outcrops of this thrust are only exposed in the northern part of the investigation area (e.g. Petković 1935; Tchoumatchenko et al. 2011) while in the central GRU the Morava dislocation is largely covered by Neogene sediments (Karamata and Krstić 1996). In the southern GRU, position and kinematics of this dislocation are poorly constrained (Dimitrijević 1997). The Vlasina Unit of the Serbo-Macedonian massif in the hangingwall of this thrust consists of a Cadomian volcano-sedimentary complex metamorphosed to greenschist facies conditions during the Variscan orogeny (Krstić and Karamata 1992; Antić et al. 2016). The Serbo-Macedonian massif is generally correlated with the Supragetic units of Romania (i.e. the highest structural level of the Carpatho-Balkan orogen; e.g. Karamata and Krstić 1996; Dimitrijević 1997; Iancu et al. 2005; Schmid et al. 2008), thrust over the Getic nappe-stack during the Early Cretaceous (e.g. Mihailescu et al. 1967; Lilov and Zagorchev 1993; Kounov et al. 2010). In the southern part of the area, the Gornjak–Ravanica Unit (Fig. 2) is thrusted by a slice of similar Palaeozoic and Mesozoic rocks belonging to the Suva Planina–Samanjac unit (Kräutner and Krstić 2003; Fig. 2), also considered to constitute a part of the Getic nappe-stack. Its relationship with the GRU is unclear and often disputed (e.g. Anđelković 1967; Antonijević et al. 1970; Veselinović et al. 1970; Krstić and Karamata 1992; Dimitrijević 1997; Kräutner and Krstić 2003).

At its eastern boundary the GRU thrusts a structurally lower part of the Getic nappe system along the Ridanj–Krepoljin dislocation zone (RKDZ). In the central part of the study area (Fig. 2) red Permian sandstones of the GRU are thrusted eastward over Early Cretaceous reef limestones of the adjacent main part of the Getic nappe system, i.e. the "Kučaj zone" (Dimitrijević 1997 and references therein) labelled as "Getic unit" in Fig. 2. Here, the RKDZ gently dips towards W-SW, with an estimated horizontal throw of ca. 10 km (Maksimović 1956; Dimitrijević 1997). The dip of RKDZ is much steeper in the southern parts of the GRU, where also a change in dip direction to E-NE was reported by Marović (2001). The RKDZ was originally

Legend:
- Quaternary sediments
- Neogene and Quaternary sediments
- Banatitic intrusions
- Timok magmatic comlex
- Gornjak-Ravanica Unit: Cretaceous
- Gornjak-Ravanica Unit: Jurassic
- Gornjak-Ravanica Unit: Triassic
- Gornjak-Ravanica Unit: Permian
- Getic Unit: Samanjac Unit
- Getic Unit: Mesozoic cover
- Getic Unit: Paleozoic basement
- Variscan granitoids
- Supragetic Unit
- Serbo-Macedonian Unit

- Thrust fault
- Undefined or strike-slip fault
- Cave
- Open pit mine

10 km

Fig. 2 Simplified geological map of the study area (after Kräutner and Krstić 2003)

active during the Late Cretaceous (Dimitrijević 1997), and was reactivated during Miocene times (Maksimović 1956).

The central parts of the GRU are structurally dominated by gentle, open and upright folds. The axes of most of these folds shallowly plunge northward with hinge lines generally striking N–S to NNW–SSE. Đoković et al. (1998) reported the presence of a piggy-back thrusting sequence with hanging wall ramps in the central part of the research area. Tectonic windows and secondary thrusts are frequent in the southern GRU. Predominantly orogen-parallel and less common orogen-perpendicular faults are better exposed in the eastern part of the GRU closer to the RKDZ thrust front.

3 Methodology

Datasets used for the paleostress analysis (a total of 1317 measurements of fault-slip data, see electronic supplementary material) were collected along four traverses through the Lower Triassic "Ravanica" limestones and the Jurassic limestones in the central GRU (Fig. 2). The northernmost traverse is located west of the Neogene basin close to the town of Kučevo (Fig. 2). The second traverse follows the course of the Mlava River, east of the town of Petrovac (Fig. 2). The third traverse is located east of the town of Despotovac (Fig. 2), whereas the fourth traverse is situated east of the town of Ćuprija (Fig. 2). Additionally, detailed structural observations were made in the open quarry Popovac near the town of Paraćin (Fig. 2), east of the town of Despotovac (Fig. 2), as well as within two caves (Fig. 2): Gaura Mare or Dubočka pećina, NE of Kučevo and Mala Bizdanja ESE of Paraćin.

Fault-slip datasets include the orientation of a discrete plane of outcrop-scale rock discontinuity, the orientation of the striation and the relative sense of movement along the observed plane, a confidence parameter of each observed shear sense indicator, as well as descriptions of the relative chronological relationships of faults and/or slip indicators (i.e. cross-cutting, overprinting). The orientations of structural data presented in this paper are displayed as dip direction/dip angle unless stated otherwise (see electronic supplementary material).

Slickenside linear structures were used as sense indicators of the highest confidence. The most common linear sense indicators were carrot-shaped wear grooves (Figs. 3b, c, e), either as sheltering trails or gouge markings (Doblas et al. 1997) and some gouging-grain grooves

(Doblas 1998) with asperity ploughing (Means 1987). Another commonly observed type of high confidence sense indicators were calcite fibres growths (Figs. 3a, f; Petit 1987). Less commonly observed slip indicators were asymmetric grains with polished lee sectors (Fig. 3Aa), spall marks with congruent steps and cm-scale synthetic fractures in upper part (Fig. 3h; Doblas et al. 1997), lunate fractures formed between fault plane and R shears (Fig. 3Ba; Petit 1987), knobby elevations with steep lee side (Fig. 3g) and plucking markings with leeward oriented concavities (Doblas 1998). Joints and tension gashes, often with calcite filling (Fig. 3d, e, g), were treated as low-confidence indicators for slip direction. One of the most important quality criteria for fault-slip analysis was a type of slip indicator (Sperner and Zweigel, 2010). Datasets in which slip was determined using slickensides were valued with the highest quality factor (1.0). Tension joints, conjugate planes or tension joints along movement planes were assumed to have the quality factor of 0.5, whereas shear joints were attributed with the quality rating of 0.25 and were taken into consideration only when slickensides were absent.

Calculation of reduced paleostress tensors and visualisation of results were completed using the Tectonics FP (TFP) software (Ortner et al. 2002). After automatic correction of fault-slip datasets (i.e. correcting for measurement errors causing slip indicator to plot away from the fault plane), their preliminary grouping was carried out on the basis of geometry (the orientation of fault planes and slip directions), taking into account evidence of reactivation and absolute or relative age (especially the recent and currently active systems; Sect. 4).

The reduced paleostress tensors were calculated using the numerical dynamic analysis (NDA; Spang 1972; Sperner and Ratschbacher 1994), or the Direct Inversion Method (INV; Angelier 1979). From the relative abundance of superimposed kinematic indicators (e.g. cross-cutting of grooves, mineral overgrowth, non-linear shear sense indicators, oblique slip, etc.) and frequent evidence of "non-Andersonian" oblique slip along observed fault planes, it was possible to distinguish a significant population of reactivated faults. Since the INV method yields accurate results for at least four datasets with variably oriented fault planes, this method was preferred when solving tensors for groups with reactivated datasets. By contrast, the NDA method is effective only if analysed datasets consist of faults formed in relatively homogeneous rocks according to the Mohr–Coulomb fracture criterion. Therefore, this method was used only when groups of datasets comprised newly-formed faults and conjugate fault systems.

Tectonic regimes associated with specific paleostress tensors were identified by the stress axis with sub-vertical

Table 1 Results of the paleostress calculations

Field point	Longitude	Latitude	Tectonic tensor	Inversion method	Number of used datasets	σ1	σ2	σ3	R	Deformational phase
K1	21,635	44,492	K1-1	NDA	4	279/72	136/15	043/10	0.5003	D2
			K1-2	NDA	6	059/34	318/16	207/51	0.4984	D1
K2	21,642	44,484	K2-1	NDA	12	163/00	073/59	253/31	0.5061	D2
			K2-2	NDA	14	217/09	344/75	125/12	0.6093	D2
			K2-3	NDA	10	204/34	062/49	308/19	0.5201	D2
			K2-4	NDA	23	010/70	190/20	100/00	0.2678	D2
			K2-5	NDA	9	054/31	297/37	172/38	0.5284	D1
			K2-6	NDA	4	090/00	359/84	180/06	0.4979	D1
			K2-7	NDA	8	098/76	257/13	348/05	0.5588	D1
K3	21,639	44,491	K3-1	NDA	28	330/33	131/55	234/09	0.5079	D2
			K3-2	INV	43	202/36	313/26	070/42	0.3735	D2
			K3-3	NDA	27	264/22	113/65	359/10	0.6037	D1
			K3-4	NDA	40	061/80	272/09	181/05	0.6081	D1
G1	21,559	44,261	G1-1	NDA	28	208/26	332/49	102/29	0.4479	D2
			G1-2	NDA	25	186/33	083/19	328/51	0.5317	D2
			G1-3	INV	18	197/37	328/41	084/27	0.4745	D2
			G1-4	NDA	16	126/34	217/02	310/56	0.3312	D1
			G1-5	NDA	13	104/13	225/66	009/20	0.5191	D1
			G1-6	NDA	16	046/24	247/65	140/08	0.5046	D1
			G1-7	NDA	4	047/32	165/37	289/37	0.4972	D1
			G1-8	INV	28	082/49	244/39	342/09	0.3572	D1
			G1-9	NDA	27	045/06	144/55	311/34	0.4745	D1
G2	21,552	44,260	G2-1	NDA	11	178/26	351/64	086/02	0.4857	D2
			G2-2	NDA	24	343/02	248/66	074/24	0.5045	D2
			G2-3	INV	8	032/17	131/29	276/56	0.5841	D2
			G2-4	NDA	9	295/24	036/23	164/56	0.556	D1
			G2-5	NDA	14	014/75	142/10	234/12	0.29	D1
			G2-6	NDA	26	061/78	298/06	207/10	0.4946	D1
			G2-7	NDA	43	039/14	274/66	134/19	0.4489	D1
			G2-8	NDA	27	339/02	244/68	070/22	0.4863	D1

Table 1 (continued)

Field point	Longitude	Latitude	Tectonic tensor	Inversion method	Number of used datasets	σ1	σ2	σ3	R	Deformational phase
G3	21,548	44,265	G3-1	NDA	18	005/18	137/64	269/18	0.5633	D2
			G3-2	NDA	4	018/37	139/34	256/35	0.501	D2
			G3-3	NDA	12	013/82	183/08	273/01	0.5864	D2
			G3-4	NDA	8	297/35	188/26	070/44	0.5012	D1
G4	21,538	44,271	G4-1	NDA	24	181/33	329/53	080/16	0.5822	D2
			G4-2	NDA	15	350/23	244/34	107/48	0.499	D2
			G4-3	NDA	15	340/53	171/36	077/05	0.5035	D2
			G4-4	NDA	22	174/65	337/24	070/07	0.5104	D2
			G4-5	NDA	8	316/37	069/27	185/41	0.4876	D1
			G4-6	NDA	36	295/13	070/72	202/12	0.504	D1
			G4-7	NDA	20	304/86	212/00	122/04	0.2697	D1
G5	21,528	44,274	G5-1	NDA	4	223/31	058/58	317/07	0.4996	D2
			G5-2	NDA	4	192/25	283/02	017/65	0.4945	D2
			G5-3	NDA	8	215/79	105/04	015/10	0.5138	D1
G6	21,538	44,260	G6-1	NDA	6	348/50	078/00	169/40	0.3584	D2
			G6-2	NDA	9	285/12	052/71	192/15	0.481	D1
			G6-3	NDA	4	285/75	095/14	186/02	0.4981	D1
			G6-4	NDA	4	039/18	138/24	277/59	0.4884	D1
M1	21,466	44,106	M1-1	INV	13	352/07	234/75	084/13	0.1226	D2
			M1-2	INV	9	149/16	052/25	268/60	0.1333	D2
			M1-3	NDA	15	232/00	322/36	141/54	0.4819	D1
M2	21,453	44,109	M2-1	NDA	4	004/04	206/85	094/02	0.4994	D2
			M2-2	INV	18	169/04	066/73	260/16	0.6672	D2
			M2-3	INV	62	156/00	246/16	065/74	0.782	D2
			M2-4	INV	30	254/31	055/58	159/09	0.2292	D1
			M2-5	INV	25	321/85	094/04	184/04	0.1026	D1
M3	21,484	44,123	M3-1	NDA	10	172/20	275/31	055/52	0.5394	D2
			M3-2	NDA	10	273/17	127/70	006/10	0.6287	D1
			M3-3	NDA	13	057/28	254/61	151/07	0.5488	D1

Table 1 (continued)

Field point	Longitude	Latitude	Tectonic tensor	Inversion method	Number of used datasets	σ1	σ2	σ3	R	Deformational phase
R1	21,503	43,977	R1-1	NDA	5	345/ 18	204/ 68	080/ 13	0.5038	D2
			R1-2	INV	15	041/ 14	139/ 30	289/ 57	0.6604	D2
			R1-3	INV	11	007/ 41	108/ 12	211/ 47	0.3783	D2
			R1-4	INV	20	200/ 63	093/ 09	359/ 25	0.2127	D1
			R1-5	NDA	5	033/ 02	125/ 39	301/ 51	0.5074	D1
R2	21,516	43,975	R2-1	INV	29	355/ 27	223/ 52	098/ 24	0.241	D2
			R2-2	NDA	10	071/ 22	209/ 62	334/ 17	0.488	D1
			R2-3	NDA	9	276/ 06	019/ 66	184/ 23	0.494	D1
			R2-4	NDA	10	103/ 14	348/ 58	200/ 28	0.4878	D1
			R2-5	INV	20	219/ 15	125/ 14	354/ 69	0.1511	D2
R3	21,523	43,973	R3-1	NDA	15	014/ 04	107/ 31	278/ 58	0.565	D2
			R3-2	NDA	17	331/ 10	083/ 66	237/ 22	0.5229	D2
			R3-3	NDA	6	305/ 19	212/ 10	095/ 69	0.5	D1
			R3-4	NDA	18	097/ 37	188/ 01	279/ 53	0.4759	D1
			R3-5	NDA	11	254/ 38	031/ 43	144/ 23	0.5077	D1
			R3-6	NDA	19	253/ 73	085/ 17	354/ 03	0.5255	D1
			R3-7	NDA	10	130/ 69	242/ 08	334/ 19	0.4616	D1
R4	21,527	43,969	R4-1	NDA	5	345/ 38	095/ 23	209/ 42	0.4995	D2
			R4-2	NDA	6	128/ 58	353/ 24	253/ 20	0.5013	D2
			R4-3	NDA	6	263/ 68	133/ 14	039/ 16	0.5069	D2
			R4-4	INV	21	024/ 19	120/ 17	249/ 64	0.4516	D1
R5	21,533	43,968	R5-1	NDA	6	258/ 15	069/ 75	168/ 02	0.5125	D1
R7	21,492	43,973	R7-1	NDA	14	358/ 15	182/ 75	089/ 01	0.4411	D2
			R7-2	NDA	19	227/ 12	105/ 68	321/ 18	0.5034	D1
			R7-3	NDA	10	089/ 18	202/ 52	347/ 33	0.4708	D1
			R7-4	NDA	5	048/ 83	248/ 06	158/ 02	0.4983	D1
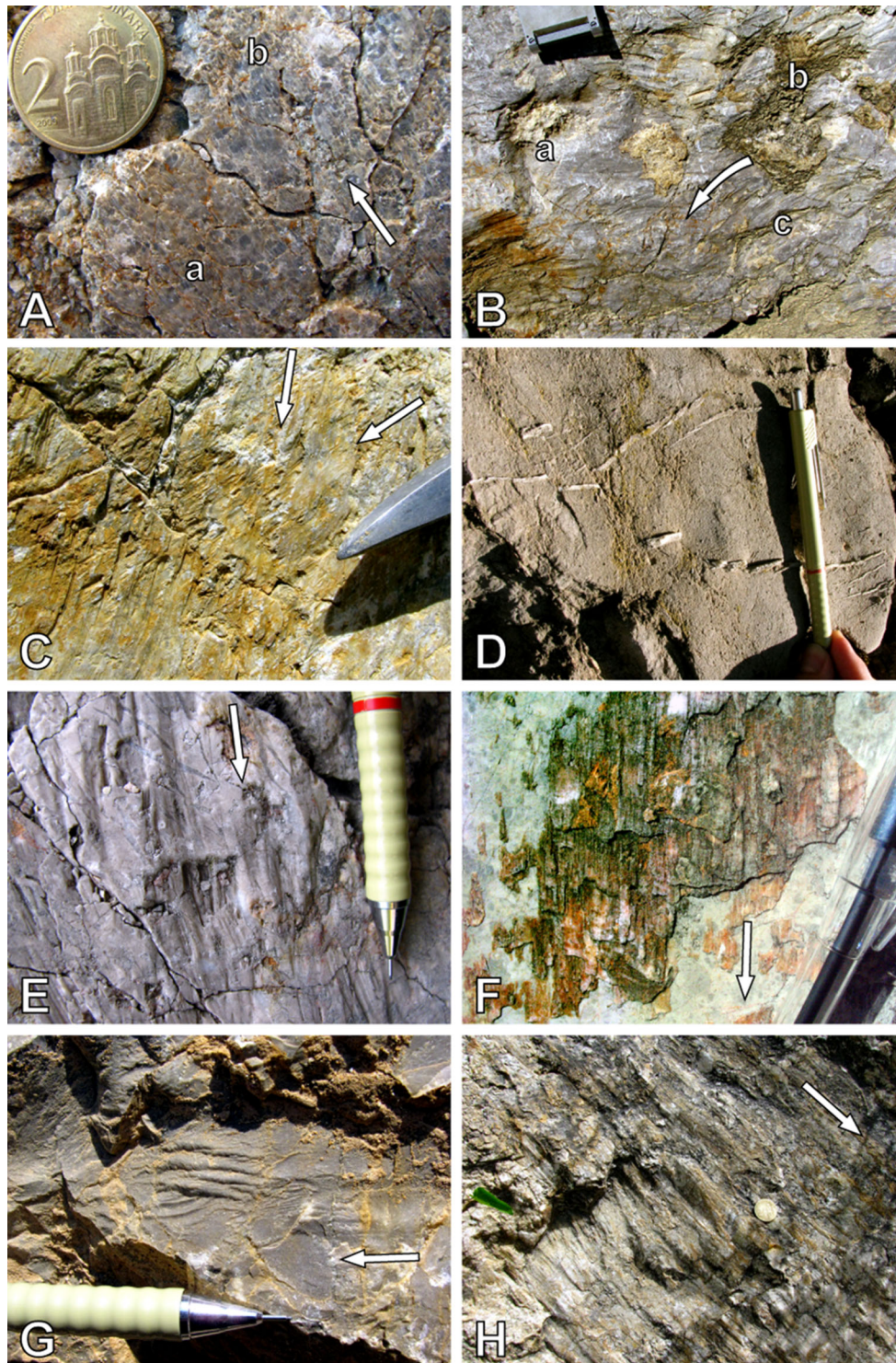
Fig. 3 Aa: Asymmetric grains (b type of Doblas et al. 1997); Ab: calcite growth, diameter of coin is 2.2 cm; Ba: lunate fracture with trailing gouge material (Petit 1987); Bb: trail material; Bc: curving grooves, compass for scale; C: crosscutting systems of „carrot-shaped" gauge markings (Doblas et al. 1997), hammer tip for scale; D; displacement of calcite-filled tension gashes along shear joints, pencil for scale; E: gouging-grain grooves (Doblas, 1998) with asperity ploughing (Means 1987), two generations of tension gashes are also visible, pencil for scale; F crystallization on the lee side of asperities (Petit 1987), pencil for scale; G: four asymmetric elevations (Doblas 1998) with tension gashes? Pencil for scale; H: spall marks and plucking markings (Doblas et al. 1997), coin for scale, arrow indicates slip sense
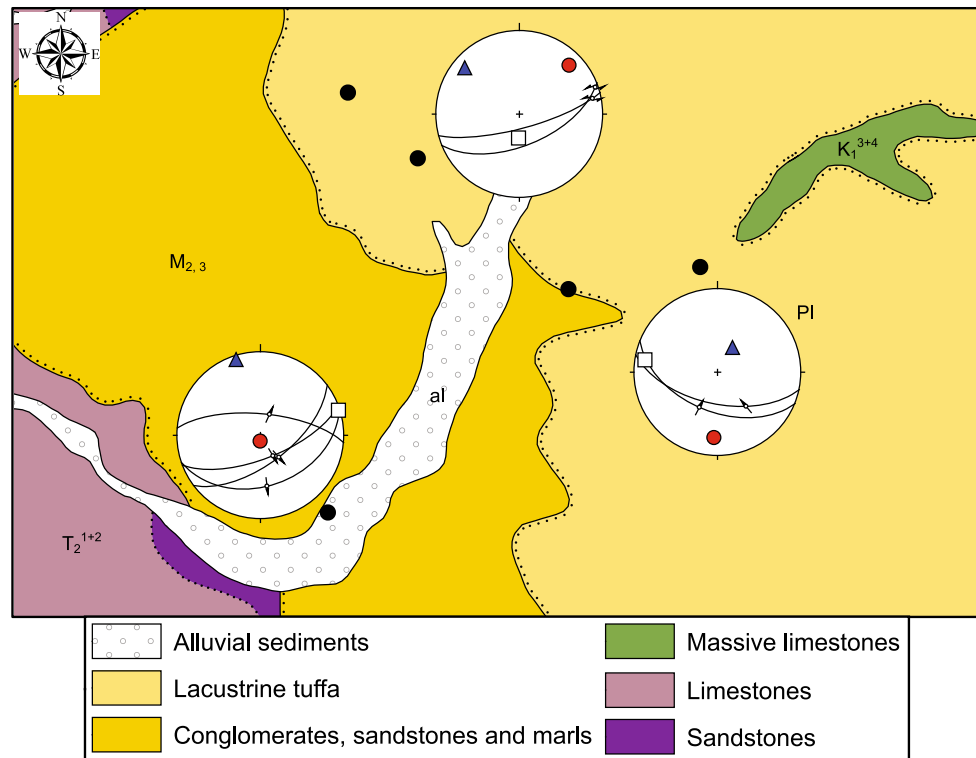
Fig. 4 Geological map of the Miocene–Pliocene sedimentary basin east of the town of Despotovac (location given on Fig. 2). Observation points are marked as black dots. Observed faults with striations orientation. (arrows indicate slip sense), as well as calculated tensors are provided in stereoplots (red circle: maximum compression; white rectangle: intermediate axis; blue triangle: extensional axis)

orientation. Thus, the vertical position of σ_1, σ_2 or σ_3 suggests extensional, strike-slip or compressional regime, respectively (Ritz 1991; Ritz and Taboada 1993). The shape of a stress-ellipsoid enables further characterization of the stress regime. It is expressed by the R parameter (ranging between 0 and 1), which describes the relative ratio between the magnitudes of the three principal stress axes (R = $\sigma_2 - \sigma_3/\sigma_1 - \sigma_3$; Etchecopar et al. 1981). Although all calculated paleostress tensors were taken into consideration regardless of the calculation method applied, the results yielded by the INV algorithm were regarded as more reliable, as the R values calculated by the NDA method bear no factual significance (Sperner and Zweigel, 2010). Many authors consider that the occurrence of extreme R values (e.g. radial compression—vertical σ_3 and $0.75 \leq R \leq 1$, or radial extension—vertical σ_1 and $0 \leq R \leq 0.25$) are quite difficult to explain in nature (e.g. Ritz and Taboada 1993; Delvaux and Sperner 2003). Consequently, calculated stress tensors indicating such extreme R values were treated as implausible and inconclusive and were ignored from further considerations.

4 Results

Based on the statistical analyses of measured fault sets and the calculation of the reduced stress tensors, two main tensor groups are distinguished (Table 1). Below, we describe these paleostress tensor groups in chronological order.

The older group comprises reduced paleostress tensors determined from the three main fault groups: (1) NNE-trending dextral faults with accompanying Riedel shear structures (a conjugate system of NE- and NW-trending strike-slip faults, as well as WNW-trending sinistral faults), (2) NW-trending reverse faults mainly dipping to NE and (3) NE-trending normal faults, dipping both to NW and SSE (see stereoplots in the electronic supplementary material). Both in map and outcrop scale, the aforementioned NNW-trending dextral faults are accompanied by Riedel structures. The Riedel structures appear as NNW- and NE-trending dextral systems (P and R shears, respectively), as well as WNW-trending sinistral faults (R' shears). The NE–SW striking normal faults were recognised as syn-sedimentary structures in the middle Miocene sediments east of the town of Despotovac (Figs. 4, 5), as well as in middle Miocene deposits of the Popovac quarry (Fig. 6). From the tensor dataset interpreted as belonging to
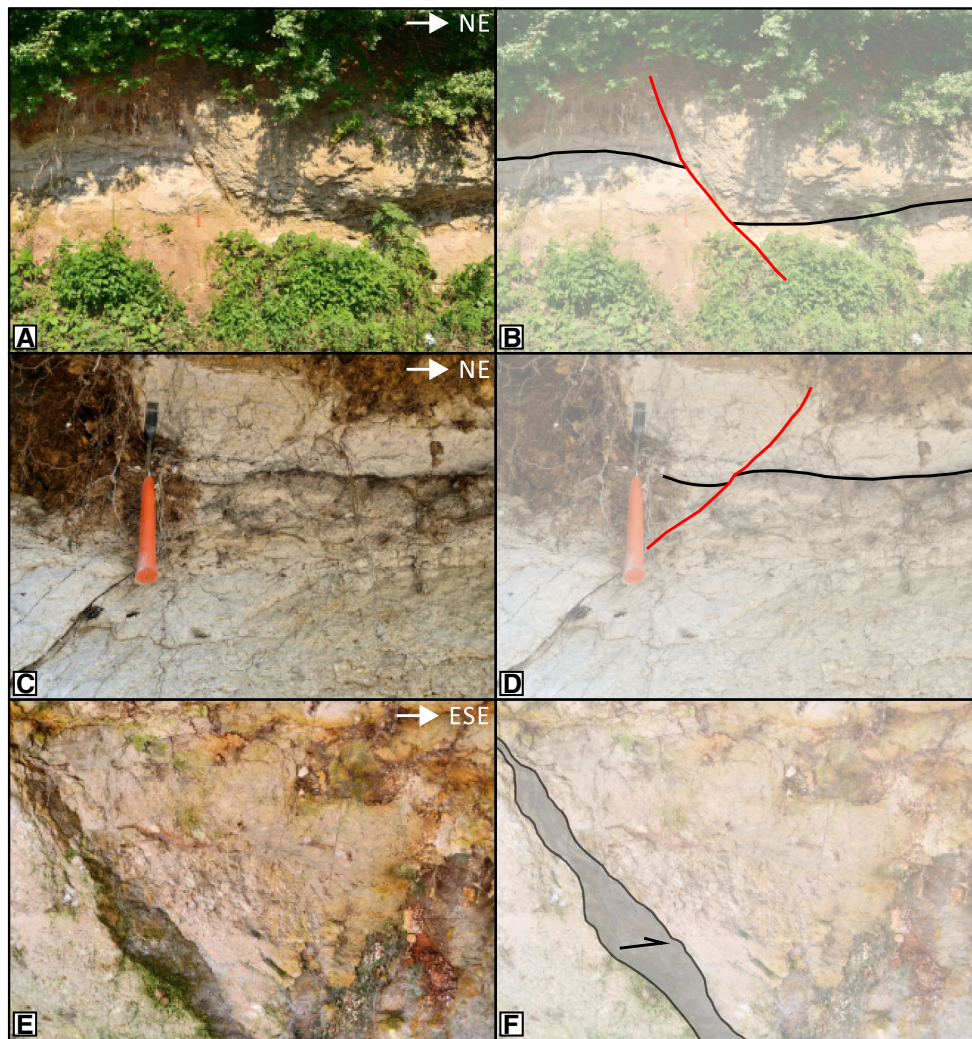
Fig. 5 Photographs indicating the interpretation of field evidences of fault activity in the area of the Miocene–Pliocene sedimentary basin east of the town of Despotovac (map on Fig. 4). **a**, **b** Synsedimentary normal fault in Middle Miocene sediments. **c**, **d** Normal faulting in Middle Miocene sediments. **e**, **f** Fault plane of a sinistral strike slip fault in Pliocene sediments

the older tectonic phase, one can distinguish three main tectonic regimes: strike-slip, compressional and extensional. The reason why we group them together in the same tectonic phase is because we regard this tectonic phase as being basically active in the strike-slip regime; the compressional and extensional regimes are regarded as being of smaller and local importance (see details discussed in Sect. 5.2). The map with the azimuth of the calculated paleostress tensor axes (Fig. 7a) indicates a generally NE–SW oriented axis of maximum compression, and a NW–SW oriented extension axis.

The younger group of paleostress tensors is calculated on the basis of several fault sets: a conjugate system of NNW-trending dextral faults and NE-trending sinistral faults, as well as N–S (NNE–SSW) striking normal faults and WNW-trending oblique reverse faults (see stereoplots in the electronic supplementary material). Fault groups

activated during this deformational phase are regarded as neotectonically and recently active (explained in Sect. 5.3). The map showing the azimuth of the calculated paleostress tensor axes (Fig. 7b) shows NNE–SSW oriented compressional axes, and WNW–ESE oriented extensional axes, again related to an overall strike-slip tectonic regime.

5 Discussion

The structural and paleostress data presented above reveal that since the Oligocene times the GRU underwent at least two stages of brittle deformation. A model of the activation of different fault systems during these two phases is given in Fig. 8.
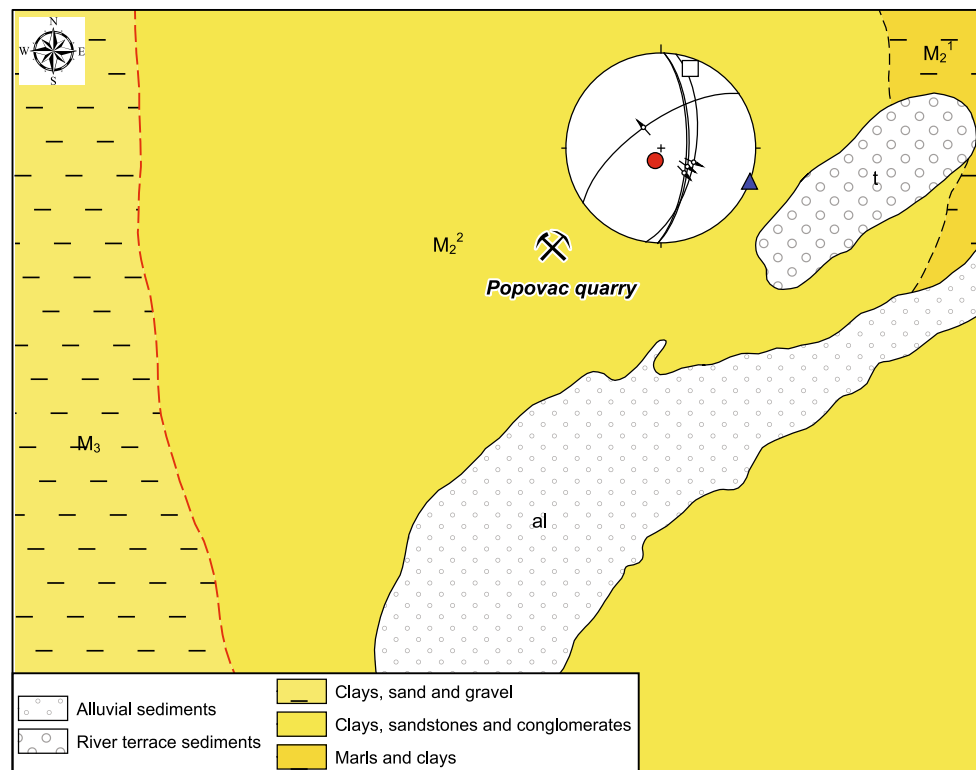
Fig. 6 Geological map of the Middle Miocene sedimentary basin east of the town of Paraćin, with the location of the Popovac quarry, where observations of fault kinematics were made. Observed synsedimentary normal faults with striations (arrow indicate slip sense), as well as calculated tensor are given in stereoplot (tensor axes: red circle: maximum compression; white rectangle: intermediate axis; blue triangle: extensional axis)

5.1 Cretaceous deformation of the Getic unit

As mentioned in the previous text the area of investigation underwent Cretaceous deformation, characterized by two main deformational phases: Early Cretaceous ('Austrian') and Late Cretaceous ('Laramian') compressional events. The Early Cretaceous deformational phase was related to the closure of the Ceahlau–Severin ocean and collision between the Dacia mega-unit and the Moesian promontory (Schmid et al. 2008; Bojar et al. 1998; Iancu et al. 2005). During this phase, the Getic nappes were formed, mainly in a ductile and semi-ductile regime, as recently reported by Krstekanić et al. (2017). The Late Cretaceous compressional phase led to the reactivation of the Getic nappes and thrusting of the Getic domain over the Danubian unit, as well as over the Moesian promontory (Iancu et al. 2005), again under a ductile to semi-ductile regime.

Taking this older history into account, as well as the fact that the main Getic thrusts were multiply active also during the Cenozoic times, we could not distinguish whether reverse faults observed only in Mesozoic sediments were active during these Cretaceous tectonic phases, or during the Cenozoic. Since these Cretaceous phases, at least in this part of the Carpatho–Balkanides, was ductile to semi-

ductile, and since we have clear evidences for activation of reverse faults during Neogene times, we exclude Cretaceous deformations to be responsible for the faulting we analysed and hence focus the discussion on the Cenozoic, i.e. post Eocene to Oligocene deformation.

5.2 Deformation phase D1: complex rotation of the Dacia mega-unit

We regard the deformational phase D1 as being related to the rotation of the Dacia mega-unit around the rigid Moesian promontory. The earliest deformational feature reported to be related to the oroclinal bending of the Dacia mega-unit is the Eocene–Oligocene orogen-parallel extension that exhumed the Danubian unit within the Southern Carpathians (Schmid et al. 1998; Maţenco and Schmid 1999; Fügenschuh and Schmid 2005). This rotation of the Dacia mega-unit was subsequently accommodated

Fig. 7 Stress tensors related to **a** deformational phase D1 and **b** D2. ▶ The locations of resulting stress tensors are given approximate to locations where fault data included in the respective calculation were recorded
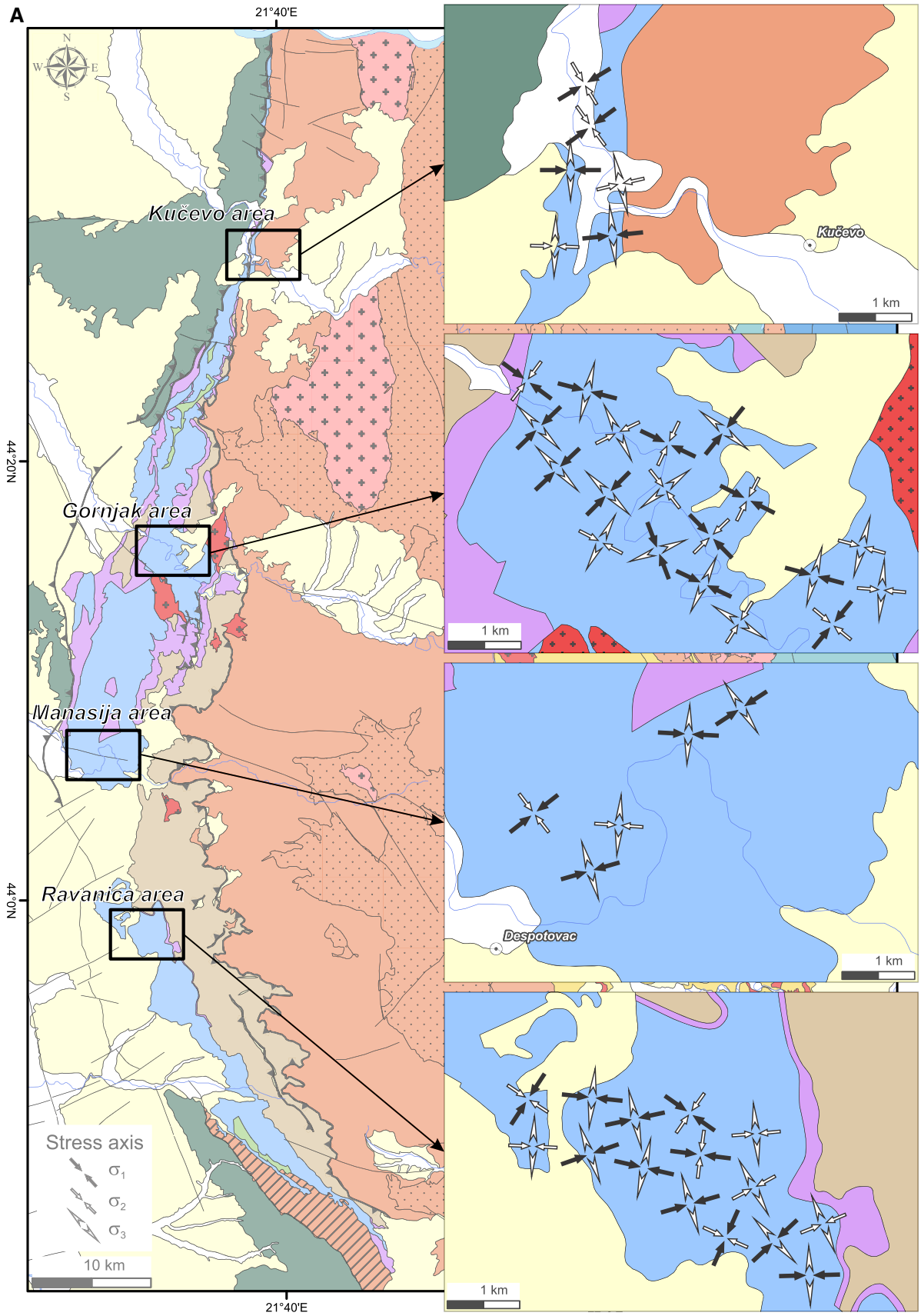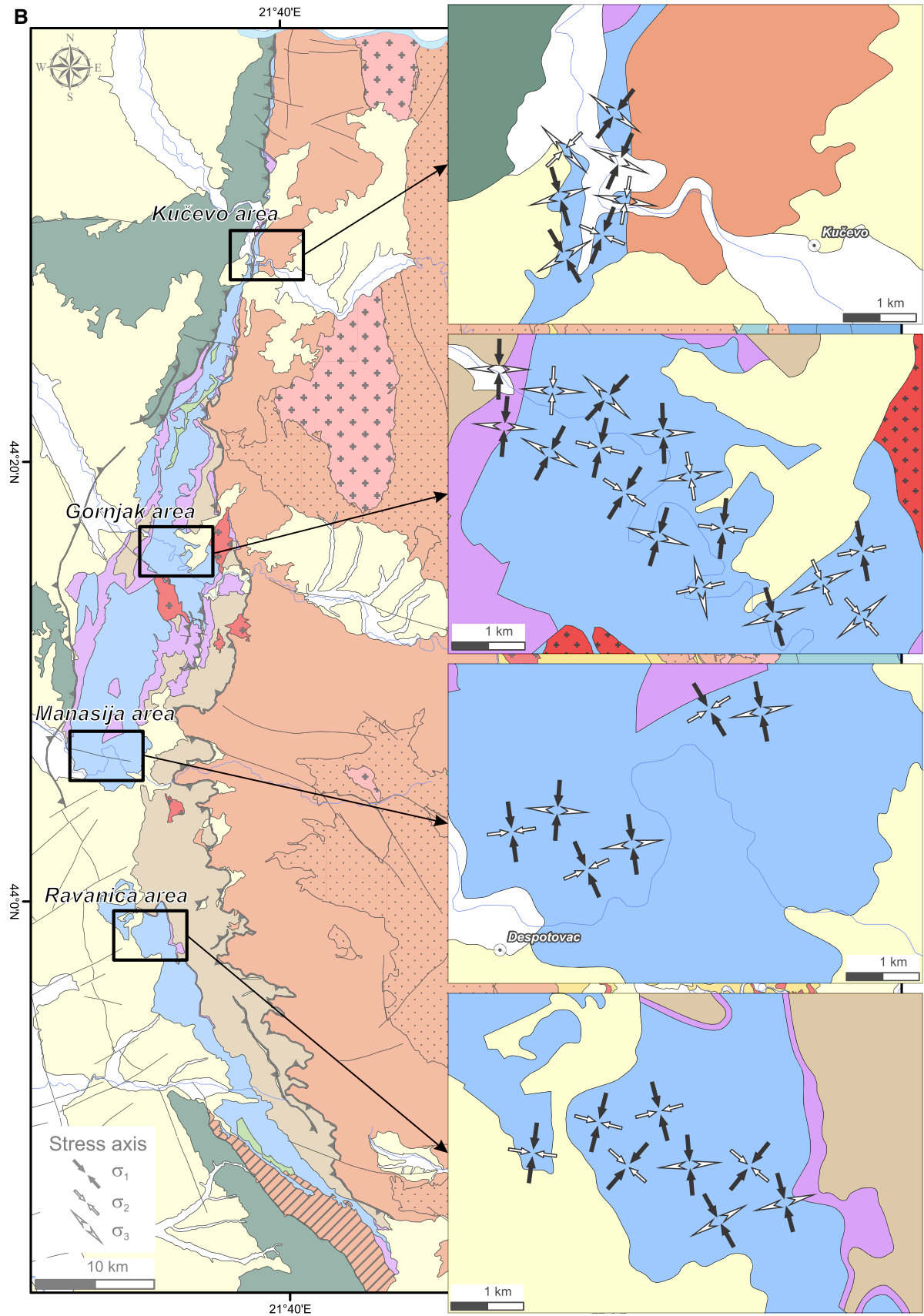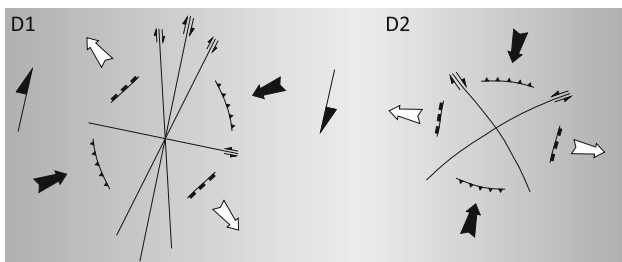
Fig. 7 continued

Fig. 8 Schematic diagram of main fault systems active during deformational phase D1 (left) and D2 (right). White arrows correspond to general direction of minimum stress axis σ_3, whereas black arrows designate the general orientation of the maximum stress axis σ_1. Orientation of σ_2 is considered to be vertical in both cases. Black half arrows in the right image represent general sense of regional shear

by the formation and activation of dextral strike-slip faults (i.e. Cerna-Jiu and Timok) during Oligocene and Miocene. Because of that, we propose that our first deformational phase started by the end of the Eocene and/or the beginning of the Oligocene.

As can be seen from the Fig. 7a (see also the stereoplots in the electronic supplementary material,) the D1 deformation phase is characterized by tensors reflecting three tectonic regimes: strike-slip, extensional and compressional. We regard this tectonic phase to be characterized by an overall strike-slip regime, leading to the activation of mainly dextral faults trending NNE–SSW and related Riedel structures. Extensional and compressional tectonic tensors are interpreted to only be locally important during

Fig. 9 Schematic sketch of oroclinal bending and clockwise rotation of the Dacia mega-unit around the Moesian promontory, and activation of dextral strike-slip faults (Cerna-Jiu and Timok), as well as the expected direction of extension during this process (white double arrows). The research area is indicated by red rectangle
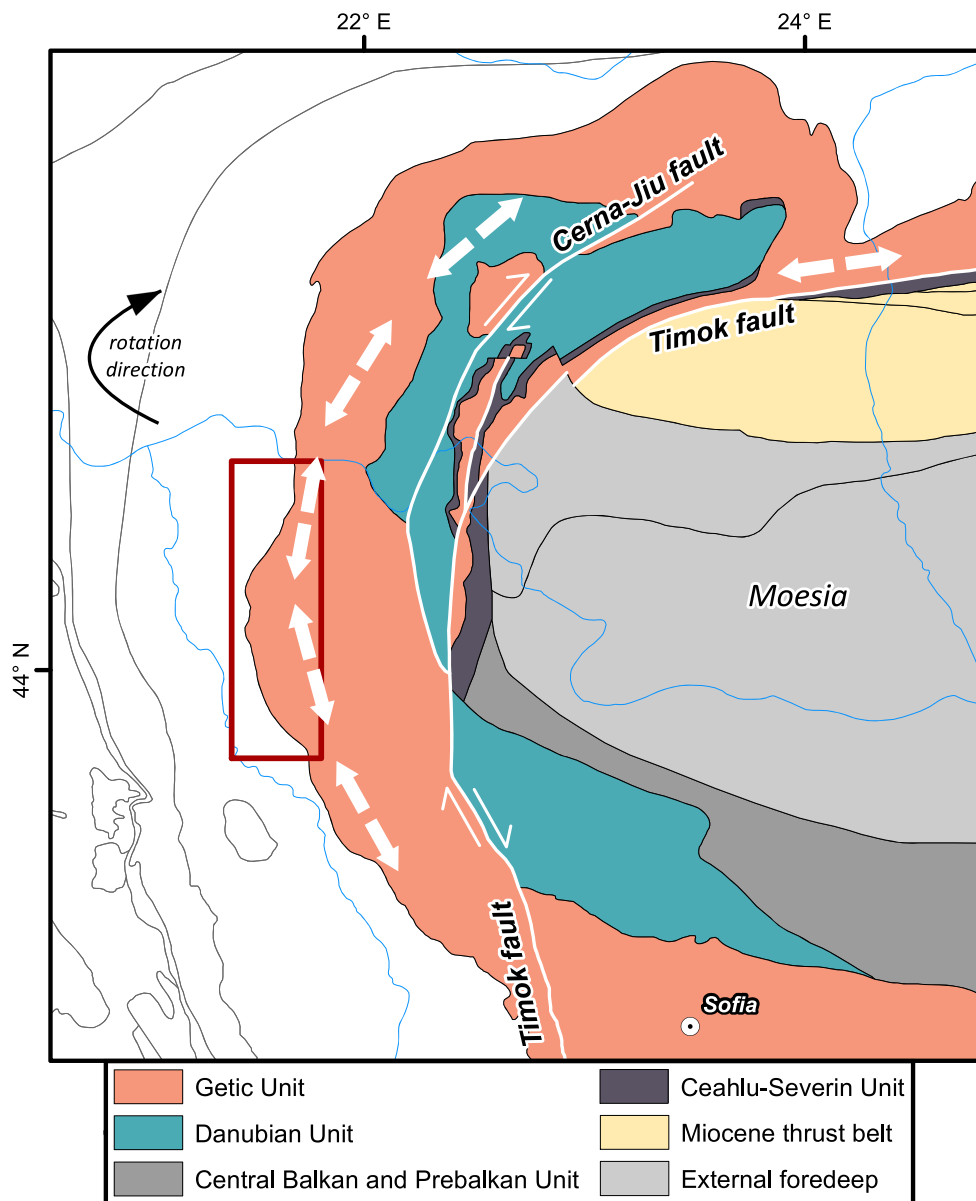
this same tectonic phase, spatially and temporally separated one from the other. We propose such an interpretation because there is no consistent field evidence for a relative chronology between normal, reverse and strike-slip faults active during this tectonic phase. Normal faults belonging to this tectonic phase can be seen to cross-cut dextral NNE-trending faults but are also seen to be cross-cut by both strike-slip and reverse faults along the entire investigated area.

The older deformational phase is characterized by a stress tensor with a generally NE–SW oriented compressional axis and generally NW–SE oriented extensional axis, acting in an overall strike-slip tectonic regime, with local domains of extension and compression within the research area. This phase activated mainly NNE–SSW striking dextral faults and related Riedel structures, and subordinately NW–SE striking reverse faults and NE–SW striking normal faults (Fig. 8). Such a stress field may be explained as being caused by dextral wrenching of the Carpatho-Balkan orogen in the contact zone with the rigid Moesian platform (Fig. 9). In such a scenario, one would expect the predominance of strike-slip faults belonging to the Cerna-Jiu and Timok fault systems. However, extensional domains (Fig. 9), as well as compressional ones, were also locally active.

Extension active during this tectonic phase was most probably responsible for the formation of all the early and middle Miocene sedimentary basins found across the entire research area (Fig. 2). Two examples of such basins are given here: a basin east of the town of Despotovac (Figs. 4, 5) and a basin east of the town of Paraćin, where the Popovac quarry is located (Fig. 6). At both localities syn-sedimentary normal faults can be seen, indicating orogen-parallel extension.

Similarly, it is supposed that local compression active during this tectonic phase, was responsible for the reactivation of thrusts and reverse faults, that were originally formed in Cretaceous times. One of the largest thrusts suspected to be reactivated during this phase is the eastern boundary of the GRU (i.e. RKDZ), that brought red Permian sandstones over the lower Miocene sediments. Reactivation of this thrust is best exposed in an underground mine exploiting Miocene coal in the central part of the research area. There, dip-slip thrusting along a gently W-SW dipping thrust plane is observed (Maksimović 1956; and own observations).

It is generally accepted that a number of transtensional to compressional events including clockwise rotations, have occurred in the Pannonian and Carpatho-Balkan domain, albeit there are different opinions regarding the exact timing of these events. In the South Carpathians, dextral transpression due to the clockwise rotation of the Tisza-Dacia block (Zweigel et al. 1998), including

transtensional and compressional domains, was reported to be of middle Oligocene to late Miocene age (Bojar et al. 1998; Maţenco et al. 2003), or alternatively, of Paleogene to early Miocene age (Linzer et al. 1998, Maţenco and Schmid 1999; Schmid et al. 2008). In the Pannonian domain, clockwise rotation occurred from Badenian to Sarmatian times, and was preceded by N–S directed compression in the middle Miocene (Csontos et al. 1991), which also affected the Apuseni Mts. (Neubauer et al. 2005). In Kraishte (SW Bulgaria), SSE–NNW directed transtension was active since the late Oligocene to earliest Miocene (Kounov et al. 2011). Also, investigations in the central Stara Planina area (Burchfiel and Nakov 2015; Kounov et al. 2018) indicate extensional/transtensional and transpressional domains active due to the oroclinal bending and rotation of the Dacia mega-unit around the rigid Moesian promontory.

5.3 Deformation phase D2: strike-slip tectonics of a locked area

The younger deformational phase in the research area involves strike-slip tectonics, with generally NNE–SSW and generally WNW–ESE oriented compressional and extensional axis, respectively. According to observations in the sedimentary basin east of Despotovac (Figs. 2, 4), where faults that were active during this tectonic phase are seen in Pliocene strata, but not in middle Miocene sediments, we suspect that this tectonic phase was not active before the end of the Late Miocene. Hence, it is regarded as being active in Pliocene to recent times.

The stress tensor of this tectonic phase activated a conjugate system of NNW-trending dextral faults and NE-trending sinistral faults, as well as N–S striking normal faults and WNW-trending oblique reverse faults (see stereoplots in the electronic supplementary material). The NNW-SSE and NE-SW striking fault systems are inferred to be neotectonically and recently active. Both fault groups are also very prominent in the cave Gaura Mare (Zlokolica-Mandić et al. 2003), where they cut speleothems and form large fault breccias that incorporate clasts of travertine cave sediments, indicating recent activity along these faults. The normal faults, generally oriented N–S (to NNE – SSW), are also neotectonically active, and this is inferred by the following three independent field observations: (1) in the Gaura Mare cave, the cave stream vertical profile is aligned along the trace of these faults (Zlokolica-Mandić et al. 2003); (2) according to the earthquake focal mechanisms, these faults are seismically active (Mladenović et al. 2014); (3) these faults cross-cut the middle Miocene syn-sedimentary faults in the Popovac quarry. Similarly, the oblique reverse faults generally striking WNW–ESE are considered to be recently active, since they cut speleothems

in the Mala Bizdanja cave (Mladenović et al. 2018). These reverse faults have also been observed in the middle Miocene sediments of the Popovac quarry and east of Despotovac, in the Pliocene sediments (Fig. 4).

The deformational phase D2 is most likely related to generally N–S directed compression also reported in the Romanian Carpathians for the period of the late Neogene (Ratschbacher et al. 1993), latest Miocene to early Pliocene (Maţenco et al. 2003), Meotian (late Tortonian) to Pleistocene (Hippolyte and Sandulescu 1996) and middle-Miocene to Pliocene (Linzer et al. 1998).

According to this model, which is corroborated by the data in the wider Pannonian–Carpatho–Balkan region (Ratschbacher et al. 1993; Hippolyte and Sandulescu 1996; Maţenco et al. 2003; Bada et al. 2007), this strike-slip tectonic phase is caused by a stress field in the area constricted between the Moesian promontory and the Adria microplate. This far-field stress is generated along the boundary between the Adriatic microplate and the Dinarides, as part of the "Adria-push" mechanism (Bada et al. 2007). This "Adria-push" generates compression oriented NE–SW to N–S, due to the counter clockwise rotation and the northward motion of the Adriatic microplate in respect to the Dinarides. In the immediate contact area of Dinarides and Adria, the generated stress field is purely compressional. However, due to the distance and geometry of tectonic units between its source and the Moesian promontory, it is conceivable that this stress field can result in a strike-slip tectonic regime, as is the case of the study area.

This strike-slip tectonic phase is considered to be active since the late Miocene up to recent times (Mladenović et al. 2014, 2018). In addition to ample field evidence presented above, we regard this phase to also be currently active, because of the contemporary seismic activity in the area which is caused by stress field that is oriented in accordance to the main stress axes (Radovanović and Pavlović 1992; Mladenović et al. 2014).

6 Concluding remarks

The results of the paleostress analysis in the GRU revealed two deformational phases that are regarded as active since Eocene–Oligocene times. The older deformational phase was most probably active from the end of the Eocene to the end of the middle Miocene, and was characterized by the activation of faults that accommodated the complex clockwise rotations of the Dacia mega-unit around the rigid Moesian promontory, located east of the research area. The younger deformational phase most likely started in the late Miocene and there is strong evidence that it is still active. It is characterized by strike-slip tectonics, resulting from the far-field stress generated by the collision of the Adriatic microplate, the Moesian promontory and the tectonic units in between.

Our results also imply that:

– The East Serbian domain of the Carpatho-Balkanides did not suffer regional extension in Oligocene to recent times, as is reported for the areas located more to the SW (e.g. Schefer et al. 2011; Stojadinovic et al. 2013) and to the SE of the study area (e.g. Kounov et al. 2010; 2011). The formation of smaller sedimentary basins that occur elsewhere along the western part of the Getic Unit was most probably controlled by local extensional/transtensional domains formed due to the clockwise rotation of the Dacia mega-unit and the activation of NNE-trending dextral faults in the region.

– Reactivation of the eastern boundary of the GRU (i.e. RKDZ) during the late Middle to Late Miocene, did not result by a regional compressional event. Rather it is an expression of a major contact zone in a locally transpressive setting due to dextral wrenching within the Getic and Danubian units in contact to the stable Moesian promontory.

References

Anđelković, M. (1967). Strukturno facijalne zone središnje i istočne Srbije. Zbornik Rudarsko-metalurškog fakulteta i Instituta za bakar 5.

Anđelković, M. (1978). *Stratigrafija Jugoslavije—paleozoik i mezozoik*. Subotica: Minerva.

Angelier, J. (1979). Determination of the mean principal directions of stresses for a given fault population. *Tectonophysics, 56,* T17–T26. https://doi.org/10.1016/0040-1951(79)90081-7.

Antić, M., Peytcheva, I., von Quadt, A., Kounov, A., Trivić, B., Serafimovski, T., et al. (2016). Alpine thermal events in the central Serbo Macedonian Massif (southeastern Serbia). *Int J Earth Sci (Geol Rundsch).* https://doi.org/10.1007/s00531-015-1266-z.

Antonijević, I., Veselinović, M., Đorđević, M., Kalenić, M., Krstić, B., Karajičić, L. (1970). Tumač za list Žagubica, Osnovna Geološka Karta 1:100000. Savezni Geološki Zavod, Belgrade.

Bada, G., Horvath, F., Dovenyi, P., Szafian, P., Windhoffer, G., & Cloetingh, S. (2007). Present-day stress field and tectonic inversion in the Pannonian Basin. *Global and Planetary Change, 58,* 165–180. https://doi.org/10.1016/j.gloplacha.2007.01.007.

Banjac, N. (2004). *Stratigrafija Srbije i Crne Gore*. Belgrade: Rudarsko-geološki fakultet.

Bojar, A.-V., Neubauer, F., & Fritz, H. (1998). Cretaceous to Cenozoic thermal evolution of the southwestern South

Carpathians: evidence from fission-track thermochronology. *Tectonophysics, 297,* 229–249.

Burchfiel, B. C., & Nakov, R. (2015). The multiply deformed foreland fold-thrust belt of the Balkan orogen, northern Bulgaria. *Geosphere, 11*(2), 463–490. https://doi.org/10.1130/GES01020.1.

Csontos, L., Tari, G., Bergerat, F., & Fodor, L. (1991). Evolution of the stress fields in the Carpatho—Pannonian area during the Neogene. *Tectonophysics, 199,* 73–91.

Cvetković, V., Prelević, D., & Schmid, S. (2016). Geology of South-Eastern Europe. In P. Papić (Ed.), *Mineral and thermal waters of Southeatern Europe. Environmental Earth sciences*. Cham: Springer.

Delvaux, D., & Sperner, B. (2003). New aspects of tectonic stress inversion with reference to the TENSOR program. *Geological Society SP, 212,* 75–100. https://doi.org/10.1144/GSL.SP.2003.212.01.06.

Dimitrijević, M. D. (1997). *Geology of Yugoslavia*. Belgrade: Geological Institute GEMINI.

Doblas, M. (1998). Slickenside kinematic indicators. *Tectonophysics, 295,* 187–197. https://doi.org/10.1016/S0040-1951(98)00120-6.

Doblas, M., Mahecha, V., Hoyos, M., & López-ruiz, J. (1997). Slickenside and fault surface kinematic indicators on active normal faults of the Alpine Betic Cordilleras, Granada, southern Spain. *Journal of Structural Geology, 19,* 159–170. https://doi.org/10.1016/S0191-8141(96)00086-7.

Đoković, I., Marović, M., Toljić, M. (1998). Gravitaciona navlačenja Gornjačko-suvoplaninskog parahtona između Mlave i Krupaje. Zapisnici SGD za 1992, 1993, 1994, 1995, 1996 i 1997. godinu, 19–21.

Etchecopar, A., Vasseur, G., & Daignieres, M. (1981). An inverse problem in microtectonics for the determination of stress tensors from fault striation analysis. *Journal of Structural Geology, 3,* 51–65. https://doi.org/10.1016/0191-8141(81)90056-0.

Fügenschuh, B., & Schmid, S. (2005). Age and significance of core complex formation in a very curved orogen: Evidence from fission track studies in the South Carpathians (Romania). *Tectonophysics, 404,* 33–53. https://doi.org/10.1016/j.tecto.2005.03.019.

Hippolyte, J.-C., & Sandulescu, M. (1996). Paleostress characterization of the "Wallachian phase" and its type area (southeastern Carpathians, Romania). *Tectonophysics, 263,* 235–248.

Iancu, V., Berza, T., Seghedi, A., Gheuca, I., & Hann, H.-P. (2005). Alpine polyphase tectono-metamorphic evolution of the South Carpathians: A new overview. *Tectonophysics, 410,* 337–365. https://doi.org/10.1016/j.tecto.2004.12.038.

Karamata, S., & Krstić, B. (1996). Terranes of Serbia and neighbouring areas. In V. Knežević-Đorđević & B. Krstić (Eds.), *Terranes of Serbia* (pp. 25–40). Belgrade: Faculty of Mining and Geology, University of Belgrade.

Kounov, A., Burg, J.-P., Bernoulli, D., Seward, D., Ivanov, Z., Dimov, D., et al. (2011). Paleostress analysis of Cenozoic faulting in the Kraishte area, SW Bulgaria. *Journal of Structural Geology, 33,* 859–874. https://doi.org/10.1016/j.jsg.2011.03.006.

Kounov, A., Gerdjikov, I., Vangelov, D., Balkanska, E., Lazarova, A., Georgiev, S., et al. (2018). First thermochronological constraints on the Cenozoic extension along the Balkan fold-thrust belt (Central Stara Planina Mountains, Bulgaria). *International Journal of Earth Sciences, 107,* 1515–1538. https://doi.org/10.1007/s00531-017-1555-9.

Kounov, A., Seward, D., Burg, J.-P., Bernoulli, D., Ivanov, Z., & Handler, R. (2010). Geochronological and structural constraints on the Cretaceous thermotectonic evolution of the Kraishte zone, western Bulgaria. *Tectonics, 29,* TC2002. https://doi.org/10.1029/2009tc002509.

Kräutner, H. G., Krstić, B. (2003). Geological map of the Carpatho-Balkanides between Mehadia, Oravita, Niš and Sofia. Geoinstitut, Belgrade.

Krstekanić, N., Stojadinović, U., Kostić, B., & Toljić, M. (2017). Internal structure of the Supragetic Unit basement in the Serbian Carpathians and its significance for the late Early Cretaceous nape-stacking. *Annales Geologiques de la Peninsule Balkanique, 78,* 1–15. https://doi.org/10.2298/GABP1778001K.

Krstić, N., & Karamata, S. (1992). Terani u Karpato-Balkanidima istočne Srbije. *Zapisnici SGD jubilarna knjiga, 1891–1991,* 57–69.

Lilov, P., & Zagorchev, I. S. (1993). K-Ar data for the deformation and low-grade metamorphism in Permian and Triassic red beds in SW Bulgaria. *Geologica Balcanica, 23,* 46.

Linzer, H.-G., Frisch, W., Zweigel, P., Girbacea, R., Hann, H.-P., & Moser, F. (1998). Kinematic evolution of the Romanian Carpathians. *Tectonophysics, 297,* 133–156.

Maksimović, B. V. (1956). Geološki i tektonski odnosi ugljonosnog terena Senjsko-Resavskih rudnika i njegovog oboda. Naučno delo, Belgrade.

Marović, M. (2001). Geologija Srbije i Crne Gore (Geology of Serbia and Montenegro), unpublished.

Maţenco, L., Bertotti, G., Cloetingh, S., & Dinu, C. (2003). Subsidence analysis and tectonic evolution of the external Carpathian—Moesian Platform during Neogene times. *Sedimentary Geology, 156,* 71–94.

Maţenco, L., & Schmid, S. (1999). Exhumation of the Danubian nappes system (South Carpathians) during the Early Tertiary: Inferences from kinematic and paleostress analysis at the Getic/Danubian nappes contact. *Tectonophysics, 314,* 401–422.

Means, W. D. (1987). A newly recognized type of slickenside striation. *Journal of Structural Geology, 9,* 585–590. https://doi.org/10.1016/0191-8141(87)90143-X.

Mihailescu, N., Dimitrijević, M. D., Dimitrijević, M. N. (1967). Les fossiles dans le flysch, in: Reports. Presented at the VIII Congress of CBGA, Serbian Geological Society, Belgrade, pp. 371–378.

Mladenović, A., Mandić, M., Ćalić, J., Gajović, V. (2018). Recent tectonic processes of the southwestern part of the Getic nappe system in Eastern Serbia—Evidences from the cave Mala Bizdanja on Samanjac Mts. Proceedings of the 17th Congress of Geologists of Serbia, pp. 169–170.

Mladenović, A., Trivić, B., Antić, M., Cvetković, V., Pavlović, R., Radovanović, S., et al. (2014). The recent fault kinematics in the westernmost part of the Getic nappe system (Eastern Serbia): evidence from fault slip and focal mechanism data. *Geologica Carpathica, 65*(2), 147–161. https://doi.org/10.2478/geoca-2014-0011.

Neubauer, F., Lips, A., Kouzmanov, K., Lexa, J., & Ivascanu, P. (2005). Subduction, slab detachment and mineralization: The Neogene in the Apuseni Mountains and Carpathians. *Ore Geology Reviews, 27,* 13–44. https://doi.org/10.1016/j.oregeorev.2005.07.002.

Ortner, H., Reiter, F., & Acs, P. (2002). Easy handling of tectonic data: The programs TectonicVB for Mac and TectonicsFP for Windows[TM]. *Computers & Geosciences, 28,* 1193–1200. https://doi.org/10.1016/S0098-3004(02)00038-9.

Petit, J. P. (1987). Criteria for the sense of movement on fault surfaces in brittle rocks. *Journal of Structural Geology, 9,* 597–608. https://doi.org/10.1016/0191-8141(87)90145-3.

Petković, V. K. (1935). *Geologija istočne Srbije, Posebna izdanja Srpske akademije nauka*. Belgrade: Srpska Kraljevska Akademija.

Radovanović, S., & Pavlović, R. (1992). Some aspects of earthquake generation in the area of Svilajnac—Žagubica. *Annales Geologiques de la Peninsule Balkanique, 56*(2), 43–60. **(in Serbian)**.

Ratschbacher, L., Linzer, H.-G., Moser, F., Strusievicz, R.-O., Bedelean, H., Har, N., et al. (1993). Cretaceous to Miocene thrusting and wrenching along the central south Carpathians due to a corner effect during collision and orocline formation. *Tectonics, 12*(4), 855–873. https://doi.org/10.1029/93TC00232.

Ritz, J. F. (1991). Evolution du champ de contraintes dans les Alpes du Sud depuis la fin de l'Oligocène: Implications sismotectoniques (PhD thesis). Université Montpellier II—Sciences et Techniques du Languedoc, Montpellier.

Ritz, J. F., & Taboada, A. (1993). Revolution stress ellipsoids in brittle tectonics resulting from an uncritical use of inverse methods. *Bulletin de la Société géologique de France, 164,* 519–531.

Schefer, S., Cvetković, V., Fügenschuh, B., Kounov, A., Ovtcharova, M., Schaltegger, U., et al. (2011). Cenozoic granitoids in the Dinarides of southern Serbia: age of intrusion, isotope geochemistry, exhumation history and significance for the geodynamic evolution of the Balkan Peninsula. *International Journal of Earth Sciences (Geol Rundsch), 100,* 1181–1206. https://doi.org/10.1007/s00531-010-0599-x.

Schmid, S. M., Bernoulli, D., Fügenschuh, B., Maţenco, L., Schefer, S., Schuster, R., et al. (2008). The Alpine-Carpathian-Dinaridic orogenic system: Correlation and evolution of tectonic units. *Swiss Journal of Geosciences, 101,* 139–183. https://doi.org/10.1007/s00015-008-1247-3.

Schmid, S. M., Berza, T., Diaconescu, V., Froitzheim, N., & Fügenschuh, B. (1998). Orogen-parallel extension in the Southern Carpathians. *Tectonophysics, 297,* 209–228.

Sikošek, B. (1955). Einige geotektonische beobachtungen im Ostteil Ostserbiens. Recueil des travaux de l'institut de geologie. *Jovan Žujović, 8,* 11–19.

Spang, J. H. (1972). Numerical method for dynamic analysis of calcite twin lamellae. *Geological Society of America Bulletin, 83,* 467–472. https://doi.org/10.1130/0016-7606(1972)83%5b467:NMFDAO%5d2.0.CO;2.

Sperner, B., & Ratschbacher, L. (1994). A Turbo Pascal program package for graphical presentation and stress analysis of calcite deformation. *Z. Dtsch. Geol. Ges., 145,* 414–423.

Sperner, B., & Zweigel, P. (2010). A plea for more caution in fault–slip analysis. *Tectonophysics, 482,* 29–41. https://doi.org/10.1016/j.tecto.2009.07.019.

Stojadinovic, U., Maţenco, L., Andriessen, P. A. M., Toljić, M., & Foeken, J. P. T. (2013). The balance between orogenic building and subsequent extension during the Tertiary evolution of the NE Dinarides: Constraints from low-temperature thermochronology. *Global and Planetary Change, 103,* 19–38. https://doi.org/10.1016/j.gloplacha.2012.08.004.

Tchoumatchenko, P., Rabrenović, D., Radulović, V., Radulović, B., & Malešević, N. (2011). Trans-border (east Serbia/West Bulgaria) correlation of the morpho-tectonic structures. *Ann. Géol. Penins. Balk., 72,* 21–27. https://doi.org/10.2298/GABP1172021T.

Veselinović, M., Antonijević, I., Milošaković, V., Mićić, I., Krstić, B., Čićulić, M. (1970). Tumač za list Boljevac, Osnovna Geološka Karta 1:100000. Savezni Geološki Zavod, Belgrade.

Zlokolica-Mandić, M., Mandić, M., Stošić, P., Radoičić, B. (2003). Novija istraživanja Dubočke pećine. In Proceedings of the 4th Symposium on karst protection, Belgrade.

Zweigel, P., Ratschbacher, L., & Frisch, W. (1998). Kinematics of an arcuate fold-thrust belt: The southern Eastern Carpathians (Romania). *Tectonophysics, 297,* 177–207.